Osteoarthritis and Cartilage 27 (2019) 1557–1563

Osteoarthritis and Cartilage

Brief Report

Deleting Suppressor of Cytokine Signaling-3 in chondrocytes reduces bone growth by disrupting mitogen-activated protein kinase signaling

X. Liu † ‡ §§, A.A. D'Cruz † ‡, J. Hansen †, B.A. Croker §, K.E. Lawlor † ‡ ‖ ¶, N.A. Sims †† ‡‡, I.P. Wicks † ‡ # *

† *Inflammation Division, The Walter and Eliza Hall Institute of Medical Research, Parkville, Victoria, 3052, Australia*
‡ *Department of Medical Biology, The University of Melbourne, Parkville, Victoria, 3010, Australia*
§ *Division of Hematology/Oncology, Boston Children's Hospital, Boston, MA, 02115, USA*
‖ *Centre for Innate Immunity and Infectious Diseases, Hudson Institute of Medical Research, Clayton, Victoria, 3168, Australia*
¶ *Department of Molecular and Translational Science, Monash University, Clayton, Victoria, 3168, Australia*
# *Rheumatology Unit, Royal Melbourne Hospital, Parkville, Victoria, 3050, Australia*
†† *St. Vincent's Institute of Medical Research, Fitzroy, Victoria, 3065, Australia*
‡‡ *Department of Medicine at St Vincent's Hospital, The University of Melbourne, 3065, Australia*
§§ *University of Queensland, Diamantina Institute, Brisbane, Queensland, 4102, Australia*

ARTICLE INFO

Article history:
Received 17 October 2018
Accepted 29 May 2019

Keywords:
Cartilage
Chondrocytes
Bone and skeleton

SUMMARY

Objective: To investigate the impact of deleting Suppressor of Cytokine Signaling (SOCS)-3 (SOCS3) in chondrocytes during murine skeletal development.
Method: Mice with a conditional *Socs3* allele ($Socs3^{fl/fl}$) were crossed with a transgenic mouse expressing Cre recombinase under the control of the type II collagen promoter (*Col2a1*) to generate $Socs3^{\Delta/\Delta col2}$ mice. Skeletal growth was analyzed over the lifespan of $Socs3^{\Delta/\Delta col2}$ mice and controls by detailed histomorphology. Bone size and cortical bone development was evaluated by micro-computed tomography (micro-CT). Growth plate (GP) zone width, chondrocyte proliferation and apoptosis were assessed by immunofluorescence staining for Ki67 and TUNEL. Fibroblast growth factor receptor-3 (FGFR3) signaling in the GP was assessed by immunohistochemistry, while the effect of SOCS3 overexpression on FGFR3-driven pMAPK signaling in HEK293T cells was evaluated by Western blot.
Results: $Socs3^{\Delta/\Delta col2}$ mice of both sexes were consistently smaller compared to littermate controls throughout life. This phenotype was due to reduced long bone size, poor cortical bone development, reduced $Ki67^{+}$ proliferative chondrocytes and decreased proliferative zone (PZ) width in the GP. Expression of pMAPK, but not pSTAT3, was increased in the GPs of $Socs3^{\Delta/\Delta col2}$ mice relative to littermate controls. Overexpression of FGFR3 in HEK293T cells increased Fibroblast Growth Factor 18 (FGF18)-dependent Mitogen-activated protein kinase (MAPK) phosphorylation, while concomitant expression of SOCS3 reduced FGFR3 expression and abrogated MAPK signaling.
Conclusion: Our results suggest a potential role for SOCS3 in GP chondrocyte proliferation by regulating FGFR3-dependent MAPK signaling in response to FGF18.

Introduction

Longitudinal bone growth is driven by chondrocyte proliferation and differentiation in the growth plate (GP), which is comprised of three cell layers. Reserve zone chondrocytes replenish the proliferative zone (PZ), where chondrocytes divide along the longitudinal bone axis. Proliferating chondrocytes differentiate into hypertrophic chondrocytes that secrete factors, which promote neovascularization and mineral deposition. Hematopoietic cells and osteoblast-progenitors invade cavities left by dying chondrocytes and osteoblasts deposit bone matrix on calcified cartilage trabeculae to form mineralized bone[1].

Fibroblast growth factor receptor-3 (FGFR3) is expressed in proliferating and hypertrophic chondrocytes. Binding of FGFs to

* Address correspondence and reprint requests to: I.P. Wicks, Reid Rheumatology Laboratory, Inflammation Division, The Walter and Eliza Hall Institute of Medical Research, 1G Royal Parade, Parkville, Victoria, 3052, Australia.
E-mail address: wicks@wehi.edu.au (I.P. Wicks).

https://doi.org/10.1016/j.joca.2019.05.018

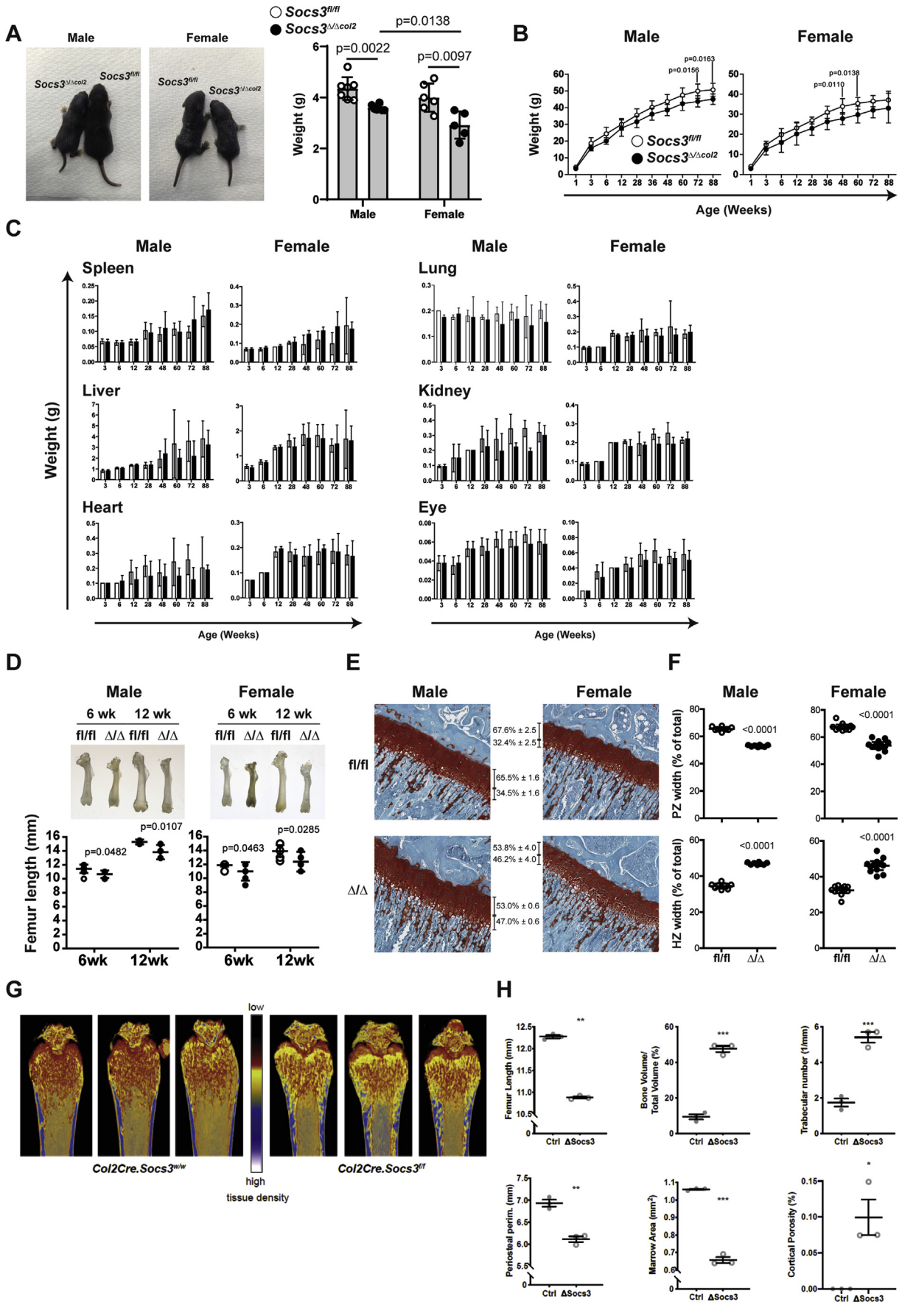
A
Male
Female
Socs3Δ/Δcol2
Socs3fl/fl
Socs3fl/fl
Socs3Δ/Δcol2
Socs3Δ/Δcol2
Socs3fl/fl
p=0.0138
p=0.0022
p=0.0097
Weight (g)
Male
Female
B
Male
Female
p=0.0163
p=0.0156
p=0.0138
p=0.0110
Weight (g)
Socs3fl/fl
Socs3Δ/Δcol2
Age (Weeks)
C
Male
Female
Male
Female
Spleen
Lung
Liver
Kidney
Heart
Eye
Weight (g)
Age (Weeks)
Age (Weeks)
D
Male
Female
6 wk
12 wk
6 wk
12 wk
fl/fl
Δ/Δ
fl/fl
Δ/Δ
fl/fl
Δ/Δ
fl/fl
Δ/Δ
Femur length (mm)
p=0.0482
p=0.0107
p=0.0463
p=0.0285
6wk
12wk
6wk
12wk
E
Male
Female
fl/fl
Δ/Δ
67.6% ± 2.5
32.4% ± 2.5
65.5% ± 1.6
34.5% ± 1.6
53.8% ± 4.0
46.2% ± 4.0
53.0% ± 0.6
47.0% ± 0.6
F
Male
Female
PZ width (% of total)
HZ width (% of total)
<0.0001
<0.0001
<0.0001
<0.0001
fl/fl
Δ/Δ
fl/fl
Δ/Δ
G
low
high
tissue density
Col2Cre.Socs3w/w
Col2Cre.Socs3f/f
H
Femur Length (mm)
Bone Volume/ Total Volume (%)
Trabecular number (1/mm)
Periosteal perim. (mm)
Marrow Area (mm²)
Cortical Porosity (%)
Ctrl
ΔSocs3

FGFR3 initiates Mitogen-activated protein kinase- (MAPK-) and Signal Transducer and Activator of Transcription (STAT)-signaling pathways. MAPK-activation inhibits chondrocyte hypertrophy, while STAT1 phosphorylation is implicated in FGFR3-induced proliferation arrest[2]. *FGFR3* mutations are associated with human dwarfism syndromes, including achondroplasia and hypochondroplasia. Achondroplasia results from a gain-of-function mutation in *FGFR3*, increasing the inhibition of endochondral ossification[2]. Similarly, patients with hypochondroplasia develop prematurely fused GPs as a result of gain-of-function *FGFR3* mutations[3]. Together, these findings suggest FGFR3-signaling regulates chondrocyte proliferation in a negative feedback loop.

The Suppressor of Cytokine Signaling (SOCS) family controls signal transduction downstream of multiple receptors. Cytokine signaling via the Janus kinase (JAK)/STAT pathway has been previously studied in the context of skeletal development. Mice with sustained gp130-mediated SHP2/ras/MAPK-activation, display reduced bone size due to abnormal chondrocyte differentiation and premature GP closure[4]. In contrast, $gp130^{Y757F/Y757F}$ mice, exhibiting sustained STAT-signaling and inhibited SOCS3-binding, have increased osteoclastogenesis and bone resorption, despite increased osteoblast numbers[4]. Mice overexpressing IL-6 develop osteopenia, which is associated with abnormal GP development, accelerated bone resorption, and impaired ossification[5]. Leukemia inhibitory factor-deficient mice display reduced bone length with abnormal chondroclast formation and osteopenia[6]. Collectively, these studies indicate JAK/STAT-signaling contributes to bone growth, but how SOCS3 specifically regulates chondrocyte responses in the GP remains undefined.

Given the importance of SOCS3 as a negative regulator of cytokine signaling, we investigated whether SOCS3 regulates chondrocyte function during bone growth. Our studies reveal deleting SOCS3 in chondrocytes reduces long bone growth, most likely due to SOCS3-mediated regulation of MAPK-signaling through FGFR3 in GP chondrocytes.

Methods

Mice

The Walter and Eliza Hall Institute (WEHI) Animal Ethics Committee approved all animal procedures. $Socs3^{\Delta/\Delta col2}$ mice (C57BL/6 background) were generated as previously described[7]. $Socs3^{fl/fl}$ mice were used as controls. Age- and sex-matched mice were (i) 6-days-of-age for GP analysis ($n = 4$) or (ii) 6-12-weeks-old for bone and GP measurements ($n = 4–8$). Separate groups of mice were aged from 1-to-88-weeks for the longevity cohort ($n = 6$-7mice/group). Sample sizes were considered sufficient for an exploratory study (Supplementary Fig. 1). All mice were fed standard rodent chow and water *ad libitum* and housed (6 mice/cage) in sawdust-lined cages.

Histomorphometry

Paraformaldehyde-fixed (PFA) knee joints were demineralized in acid, and paraffin embedded. Sections (4 μm) were stained with Safranin-O/Fast-green. Total GP width and the proliferative and hypertrophic zones (HZ) were measured at equal intervals along a 90° axis to the transverse plane of the GP and parallel to the longitudinal axis of the bone, using ImageJ. >40 measurements were obtained per section ($n = 4$ sections/GP), and the mean width determined in individual animals. The PZ and hypertrophic zone (HZ) was calculated as a percentage of total GP width.

Ethanol- and acetone-fixed femurs were treated with 1% KOH/1% glycerol then glycerol (40%, 60%, 80%, and 100%). Length was determined using Vernier calipers.

Micro-computed tomography

Formalin-fixed femora were imaged with Skyscan-1076 (Bruker). Image settings: 9 μm voxel resolution, 0.5 mm aluminum filter, 50 kV voltage and 100 μA current, exposure time, rotation 0.5°, frame averaging = 1. Images were reconstructed and analyzed using SkyScan-NRecon (v1.6.8.0), DataViewer (v1.4.4) and CT-Analyser (v1.11.8.0). Trabecular bone volume (BV) was measured in a region commencing at 7.5% of the total femur length below the distal GP towards the femoral-mid-shaft and extending for 15% of total femur length. Cortical bone, including cortical porosity was measured at a site commencing at 30% of the total femoral length towards the mid-shaft, which was 15% of the total femur length. Analysis was completed using adaptive thresholding in CT-Analyser. Thresholds were determined based on grayscale values, and calibrated to a calcium hydroxyapatite (CaHA) standard: Trabecular bone (>0.296 mg/cm^3 CaHA); Cortical bone (>0.729 mg/cm^3 CaHA).

Immunofluorescence

PFA-fixed sagittal sections (4 μm) were rehydrated and apoptosis determined using *In Situ* Apoptosis Detection Kit (Millipore). For Ki67-immunostaining, 'Antigen Unmasking Solution' (Vector-Labs) was used. Samples were permeabilized with 0.2% Triton X-100, blocked with 0.25% gelatin, incubated with rabbit-anti-mouse-Ki67 (Leica-Biosystems), and goat-anti-rabbit-Alexa546 (Invitrogen). Sections were 4',6-diamidino-2-phenylindole (DAPI) counter-stained. Cells from the entire GP were enumerated using MetaMorph (Molecular-Devices) and its in-built Multi-Wavelength Cell Scoring Application. Min/max nuclear sizes, and background thresholds were set based on example images and applied to each image.

Immunohistochemistry

Antigen retrieval was achieved using 0.05% trypsin/0.1% $CaCl_2$ for pMAPK and FGFR3, or Citrate Buffer (Lab-Vision) for pSTAT3. Sections were blocked with 10% normal goat serum (NGS), then Avidin/Biotin-block (DAKO) for pSTAT3 and FGFR3. All sections were treated with Protein-block (DAKO). Sections were incubated with pMAPK (CST, Cat#4370, [1:200]) in antibody diluent (Envision-FLEX); or in 10% NGS for FGFR3 (Abcam, Ab180906, [1:400]) and pSTAT3 (Santa-Cruz, sc-7993-R, [1:150]). Rabbit IgG (CST, Cat#3900, [1:200]) was used as the isotype control. pMAPK sections were treated with Peroxidase-block (DAKO), then EnVision+System-HRP (DAKO). pSTAT3 and FGFR3 sections were

Fig. 1. Suppressor of Cytokine Signaling (SOCS)-3-deficiency is associated with reduced long bone length. (A) Representative images and weights of 6-day-old male and female $Socs3^{\Delta/\Delta col2}$ and $Socs3^{fl/fl}$ littermate mice ($n = 24$ total, 5–7 mice/group). **(B)** Weights of male and female $Socs3^{\Delta/\Delta col2}$ and littermate mice from 1- to 88-weeks-of-age ($n = 273$ total, 6–7 mice/group). **(C)** Weights of soft tissues from male and female $Socs3^{\Delta/\Delta col2}$ and littermate mice ($n = 4$ mice/group). **(D)** Femur length in male and female $Socs3^{\Delta/\Delta col2}$ and littermate mice. Representative femurs are shown (top). ($n = 50$ total, 4–8 mice/group). **(E)** Histomorphometric analysis of Safranin-O/Fast-green stained sagittal sections of 8-week-old proximal tibial epiphysis of $Socs3^{\Delta/\Delta col2}$ and littermate mice. ($n = 16$ total, 4 mice/group). **(F)** Percentage of proliferative zone (PZ) and hypertrophic zone (HZ) width in 8-week-old male and female $Socs3^{\Delta/\Delta col2}$ and littermate mice ($n = 4$ replicates/group). **(G)** Representative micro-CT images of distal femurs from 6-week-old female $Socs3^{\Delta/\Delta col2}$ and littermate mice ($n = 12$ total, 3 mice/group). **(H)** Measurements of overall bone size, and cortical and trabecular bone microarchitecture. Bars show mean ± SD. * = $P < 0.05$ and ** = $P < 0.01$ and *** = $P < 0.001$.

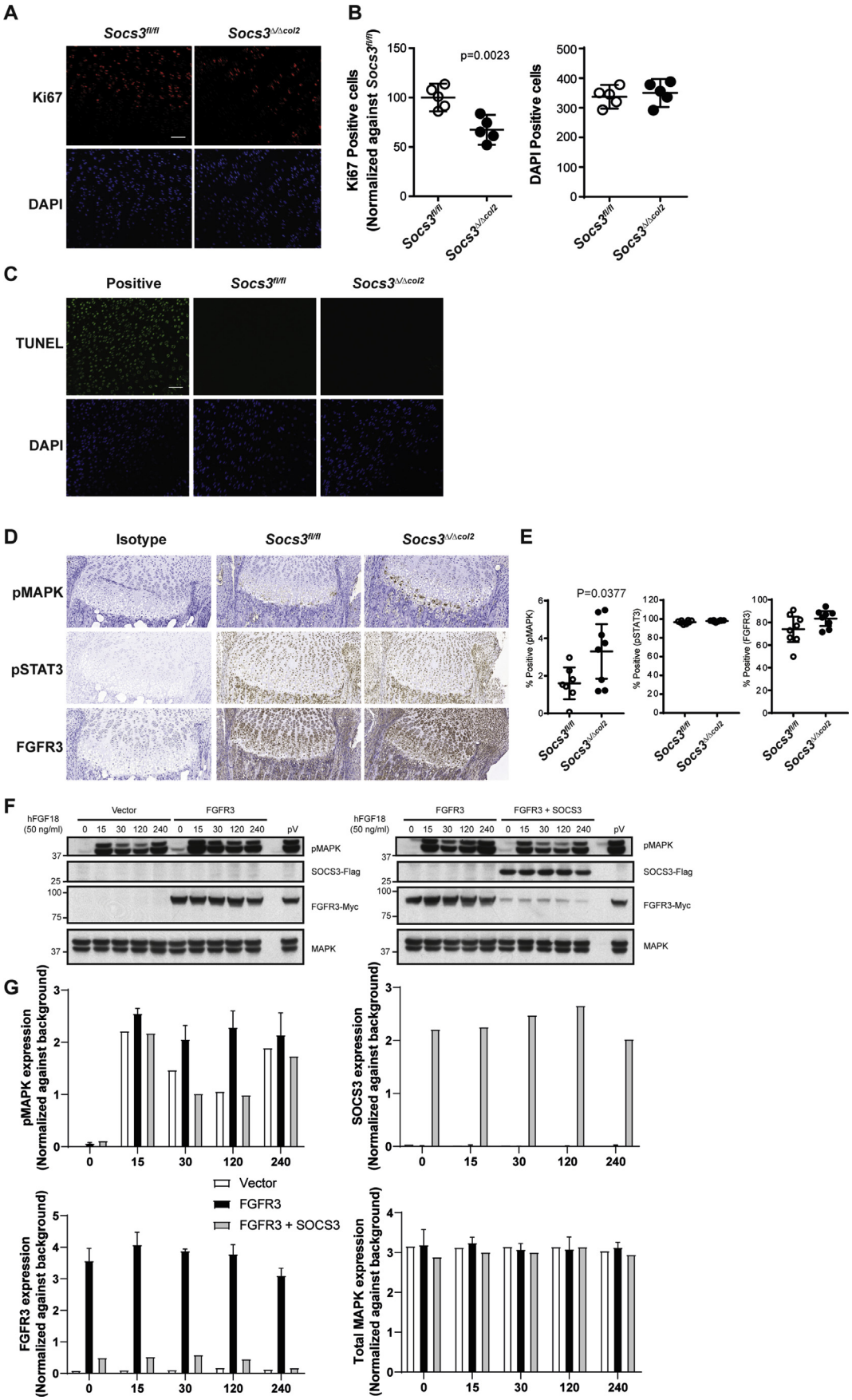
A
Socs3fl/fl
Socs3Δ/Δcol2
Ki67
DAPI
B
Ki67 Positive cells (Normalized against Socs3fl/fl)
p=0.0023
DAPI Positive cells
C
Positive
TUNEL
DAPI
D
Isotype
pMAPK
pSTAT3
FGFR3
E
P=0.0377
% Positive (pMAPK)
% Positive (pSTAT3)
% Positive (FGFR3)
F
Vector
FGFR3
FGFR3 + SOCS3
hFGF18 (50 ng/ml)
0 15 30 120 240 pV
pMAPK
SOCS3-Flag
FGFR3-Myc
MAPK
G
pMAPK expression (Normalized against background)
SOCS3 expression (Normalized against background)
FGFR3 expression (Normalized against background)
Total MAPK expression (Normalized against background)
Vector
FGFR3
FGFR3 + SOCS3

incubated with biotinylated-goat-anti-rabbit-IgG (Vector-Labs, BA-1000, [1:50]), then ABC Reagent (Vector-Labs). All were visualized with Liquid 3,3'-Diaminobenzidine+ (DAB+) (DAKO) and Hematoxylin.

Transfection and western blotting

FGFR3-MYC-tag (MYC) and SOCS3-FLAG-tag (FLAG) were subcloned into pEF-BOS. HEK293T cells in Dulbecco's Modified Eagle's Medium (DMEM) (100 U/mL penicillin, 0.1 mg/mL streptomycin and 10% Fetal Bovine Serum (FBS)) were transfected using Fugene (Promega). 48 h post-transfection, cells were treated with 50 ng/ml hFGF-18 (Peprotech) for the indicated times, lysed in NP-40 buffer (50 mM 4-(2-hydroxyethyl)-1-piperazineethanesulfonic acid (HEPES), 150 mM NaCl, 1% NP-40 and Protease inhibitor cocktail [Roche Applied Bioscience]), then centrifuged (16,060×*g*, 15min). Supernatant was combined with sodium-dodecyl-sulphate (SDS)-Laemmli buffer. Proteins were resolved by SDS-PAGE using NuPAGE-Bis-Tris precast-gels (Thermo-Fisher), transferred onto Polyvinylidene Difluoride (PVDF)-Plus-membranes (GE Water & Process Technologies), blocked in 10% skim milk, and incubated with rat-anti-FLAG (clone 9H1, gift from Prof. D.Huang & Dr. L.O'Reilly (WEHI)), or rabbit-anti-MYC (Santa-Cruz). Antibodies were visualized with goat-anti-rat-Ig-HRP (Southern-Biotech) or donkey-anti-rabbit-Ig-HRP (GE-Healthcare), and chemiluminescent substrates (GE-Healthcare) and detected by ChemiDoc-XRS (Bio-Rad). Western blots were quantified using Image Lab (v6.0.0).

Statistics

All experiments were performed using at least two technical replicates and three independent biological replicates, unless otherwise stated. Statistical analysis was performed using GraphPad-Prism. Student's *t*-test was used to compare experimental groups. Body weight curves were compared with a two-way-ANOVA-test (Bonferroni correction). Values represent mean ± 95% confidence interval, unless stated otherwise. $P < 0.05$ was considered significant.

Results

SOCS3 deletion in chondrocytes causes reduced bone size and abnormal cortical bone development

$Socs3^{\Delta/\Delta col2}$ mice were healthy, and fertile, but were consistently smaller and lighter than controls [Fig. 1(A)]. Female $Socs3^{\Delta/\Delta col2}$ mice were significantly lighter than male transgenic mice. X-gal staining confirmed Cre-recombinase expression in $R26R^{gt/+}Socs3^{\Delta/\Delta col2}$ cartilage and limited expression in the bone marrow (Supplemental Figs. 2 and 3). Longitudinal analysis of $Socs3^{\Delta/\Delta col2}$ mice showed a consistent reduction in total body weight of both sexes [Fig. 1(B)]. There was no difference in the weight of soft tissues between $Socs3^{\Delta/\Delta col2}$ and controls, indicating an effect on the skeleton [Fig. 1(C)]. We found a significant reduction in the length of the femurs from 6- and 12-week-old $Socs3^{\Delta/\Delta col2}$ mice [Fig. 1(D)]. Analysis of the GP showed a reduced PZ in 8-week-old $Socs3^{\Delta/\Delta col2}$ mice [Fig. 1(E) and (F)]. Micro-CT analysis of 6-week-old female femora confirmed the reduction in femur length in $Socs3^{\Delta/\Delta col2}$ mice, but also a reduction in overall bone size as indicated by significantly smaller periosteal perimeter and marrow area [Fig. 1(G) and (H)]. In addition, significantly diminished BV and trabecular number combined with dramatically increased cortical porosity indicated dysregulated cortical bone development in $Socs3^{\Delta/\Delta col2}$ mice. Together, these results reveal ablation of SOCS3 in chondrocytes causes decreased bone size and poor cortical bone development during skeletal growth.

SOCS3 deletion reduces growth plate chondrocyte proliferation and dysregulates FGFR3-mediated MAPK-signaling

To evaluate chondrocyte proliferation and apoptosis, Ki67- and TUNEL-immunostaining were performed on tibial GPs from 6-day-old mice. There was no difference in the total number of chondrocytes, but Ki67-staining showed reduced proliferation in $Socs3^{\Delta/\Delta col2}$ GPs [Fig. 2(A) and (B)]. TUNEL-staining showed no difference in late-stage chondrocyte apoptosis in the GPs of $Socs3^{\Delta/\Delta col2}$ and controls [Fig. 2(C)]. These data suggest SOCS3 plays a role in regulating chondrocyte proliferation at the GP during skeletal development and its deficiency causes reduced bone growth.

FGF-FGFR3-signaling plays a critical role in bone formation by inhibiting chondrocyte proliferation. To investigate the effect of SOCS3 on FGFR3-signaling in the GP, pMAPK, pSTAT3 and FGFR3 expression was assessed by immunohistochemistry. While pSTAT3 expression was comparable between $Socs3^{\Delta/\Delta col2}$ and controls, increased pMAPK staining was observed in the GPs of $Socs3^{\Delta/\Delta col2}$ mice [Fig. 2(D) and (E)].

FGFR3 and SOCS3 constructs were transfected into HEK293T cells and stimulated with hFGF18. MAPK phosphorylation was assessed by western blotting. There was reduced MAPK phosphorylation in HEK293T cells overexpressing FGFR3 and SOCS3, compared to FGFR3 alone [Fig. 2(F) and (G)]. In addition, SOCS3 overexpression appeared to reduce FGFR3 expression.

Together, these findings suggest SOCS3 negatively regulates FGFR3-signaling by limiting the duration or degree of pMAPK-activation. Dysregulation of this pathway in $Socs3^{\Delta/\Delta col2}$ chondrocytes may cause a defect in PZ chondrocytes, with premature closure of the GP reducing long bone growth during skeletal development.

Discussion

We have shown reduced body weight in one-week-old $Socs3^{\Delta/\Delta col2}$ mice, accompanied by reduced femur length, width and decreased PZ width in $Socs3^{\Delta/\Delta col2}$ GPs. Reduced chondrocyte proliferation was observed in the PZ of GPs in $Socs3^{\Delta/\Delta col2}$ mice. We provide mechanistic evidence FGFR3-signaling is altered in the absence of SOCS3, with abnormal pMAPK-activation.

FGF-FGFR-signaling inhibits bone elongation and *FGFR3* mutations cause dwarfism in humans. Negative regulation of FGFR3-signaling is not well understood. FGF-signaling activates Sprouty (SPRY) proteins, a family of MAPK phosphatases, which can inhibit FGFR-signaling by directly binding to RAF proto-oncogene serine/threonine protein kinase or c-Raf (RAF), or by competing for GRB2

Fig. 2. Reduced chondrocyte proliferation in $Socs3^{\Delta/\Delta col2}$ growth plates (GP) is associated with dysfunctional FGFR3-mediated MAPK-signaling. **(A)** Ki67 and DAPI double staining was performed on tibial joint sections collected from male 6-day-old $Socs3^{\Delta/\Delta col2}$ and littermate mice. **(B)** The presence of proliferative chondrocytes in the entire GP was determined by Ki67 and DAPI staining 6-day-old $Socs3^{\Delta/\Delta col2}$ and littermate mice. ($n = 10$ total, 5 mice/group). Scale bars (200x), 50 μm. **(C)** The apoptosis of GP chondrocytes was determined by TUNEL- and DAPI-staining in 6-day-old $Socs3^{\Delta/\Delta col2}$ and littermate mice. Sections pre-treated with 200 μg/ml DNAse I were used as a positive control. Scale bars (200x), 50 μm ($n = 8$ total, 4 mice/group). **(D)** pMAPK, pSTAT3 and FGFR3 immunohistochemistry was performed on joint sections collected from 1-week-old $Socs3^{\Delta/\Delta col2}$ and littermate mice. ($n = 15$ total, 7–8 mice/group). **(E)** Percentage of DAB positive cells in the entire GPs of $Socs3^{\Delta/\Delta col2}$ and littermate mice. **(F)** Representative Western blot image and **(G)** quantification of HEK293T-cells overexpressing both FGFR3 and SOCS3 stimulated with 50 ng/ml hFGF18 for up to 4 h ($n = 2$ experiments). Bars show mean ± SD. Cell lysates were analyzed by Western blotting for pMAPK, FLAG and MYC. Total MAPK was used as a loading control.

binding[3]. Mice overexpressing *Spry1* in chondrocytes display skeletal abnormalities resembling thanatophoric dysplasia II[8]. Extracellular signal-regulated kinase (ERK)-signaling upregulates MAPK phosphatase-3, which specifically dephosphorylates activated ERK1/2[9]. Previous studies suggested SOCS3 can bind FGFR3 and may influence receptor trafficking[10]. Our results support these observations and suggest FGFR3 ligation activates SOCS3 in a negative feedback loop during skeletal development. SOCS3 may regulate FGFR3-signaling in chondrocytes by reducing downstream MAPK-activation and preventing premature inhibition of chondrocyte proliferation. Under physiological conditions, activation of FGFR leads to internalization, followed by ubiquitination and degradation[11]. We found no difference in the proportion of FGFR3 positive chondrocytes in the GPs of $Socs3^{\Delta/\Delta col2}$ and controls. A caveat to this study is the use of transfected HEK293T cells due to the difficulty in collecting and transfecting primary GP chondrocytes. Nevertheless, it is possible SOCS3 can regulate the receptor expression per cell by binding to FGFR3 and promoting its recycling and degradation[12].

Reduced long bone size and dysregulated cortical bone formation may not be solely dependent on aberrant FGFR3-signaling in $Socs3^{\Delta/\Delta col2}$ mice. Growth hormone (GH), Insulin Growth Factor-I (IGF-I) and growth factors such as androgens also regulate endochondral ossification. SOCS2-deficient mice develop gigantism through sustained GH-induced STAT5b-signaling[13]. Disruption of SOCS3-signaling in chondrocytes may also disrupt GH- and IGF-I-induced STAT5b-signaling, with anabolic effects that may have contributed to abnormal cortical bone development. A similar phenotype of abnormal bone corticalization, but not reduced bone size, was reported in *Dmp1Cre.Socs3*$^{fl/fl}$ mice, which was both sex- and IL-6-dependent[14]. Therefore, the reduced bone size and dysregulated cortical bone development in $Socs3^{\Delta/\Delta col2}$ mice may be due to prolonged MAPK-signaling in addition to dysregulated growth factor/hormone signaling. Furthermore, SOCS3 may be deleted, to some extent, in other cells regulating bone growth and cortical development, including osteoblasts and osteoclasts[15].

The molecular mechanisms underlying common chondrodysplasias have been attributed to constitutive FGFR3 activation leading to prolonged STAT1-and MAPK-activation[2]. Prolonged STAT1-signaling can dysregulate chondrocyte proliferation via p21[2]. The MAPK pathway can inhibit chondrocyte proliferation, terminal differentiation and post-mitotic matrix synthesis, via p38 and ERK cascades[9]. Alternatively, chondrodysplasia can be meditated indirectly, by dysregulation *Ihh* and *Bmp4* signaling pathways, which regulate chondrocyte proliferation and maturation[9]. Therefore, prolonged activation of pMAPK in GP chondrocytes of $Socs3^{\Delta/\Delta col2}$ mice may inhibit bone growth by decreasing the expression of these regulators of skeletogenesis.

Our study demonstrates SOCS3 regulates chondrocyte proliferation in the GP during bone growth. While further research is required, our data indicates SOCS3 regulates FGFR3-signaling by reducing the magnitude and duration of pMAPK-activation, and possibly by altering the kinetics of FGFR3 recycling.

Author contributions

Study conception and design: XL, AAD, JH, BAC, KEL, IPW.

Acquisition, analysis and interpretation of data: XL, AAD, JH, BAC, KEL, NAS, IPW.

Writing and critical revision of article: XL, AAD, JH, BAC, KEL, NAS, IPW.

Final approval of the article: XL, AAD, JH, BAC, KEL, NAS, IPW.

XL (tommy.liu@uq.edu.au) and IPW (wicks@wehi.edu.au) take responsibility for the integrity of the work as a whole, from inception to finished article.

Competing interests

The authors have no conflicting financial interests to disclose.

Role of the funding source

Supported by the Reid Charitable Trusts, the Arthritis Foundation of Australia, the National Health and Medical Research Council of Australia (grants 1023407 and 1016647 to Dr. Wicks, and grant 1120978 to Dr. Sims) and the Victorian State Government (Operational Infrastructure Grant). I.P.W's lab has received funding from CSL and MedImmune for research on cytokine antagonists.

Acknowledgements

We thank Nicole C. Walsh, Brett A. Tonkin and Ryan Galea for helpful discussions and advice, and Narelle E. McGregor for technical assistance. We also thank Warren S. Alexander for providing *Socs3*$^{fl/fl}$ mice.

Supplementary data

Supplementary data to this article can be found online at https://doi.org/10.1016/j.joca.2019.05.018.

References

1. Mackie EJ, Tatarczuch L, Mirams M. The skeleton: a multifunctional complex organ: the growth plate chondrocyte and endochondral ossification. J Endocrinol 2011;211(2):109–21.
2. Ornitz DM, Marie PJ. Fibroblast growth factor signaling in skeletal development and disease. Genes Dev 2015;29(14):1463–86.
3. Teven CM, Farina EM, Rivas J, Reid RR. Fibroblast growth factor (FGF) signaling in development and skeletal diseases. Genes Dis 2014;1(2):199–213.
4. Sims NA, Jenkins BJ, Quinn JM, Nakamura A, Glatt M, Gillespie MT, *et al.* Glycoprotein 130 regulates bone turnover and bone size by distinct downstream signaling pathways. J Clin Investig 2004;113(3):379–89.
5. De Benedetti F, Rucci N, Del Fattore A, Peruzzi B, Paro R, Longo M, *et al.* Impaired skeletal development in interleukin-6-transgenic mice: a model for the impact of chronic inflammation on the growing skeletal system. Arthritis Rheum 2006;54(11):3551–63.
6. Poulton IJ, McGregor NE, Pompolo S, Walker EC, Sims NA. Contrasting roles of leukemia inhibitory factor in murine bone development and remodeling involve region-specific changes in vascularization. J Bone Miner Res 2012;27(3):586–95.
7. Liu X, Croker BA, Campbell IK, Gauci SJ, Alexander WS, Tonkin BA, *et al.* Key role of suppressor of cytokine signaling 3 in regulating gp130 cytokine-induced signaling and limiting chondrocyte responses during murine inflammatory arthritis. Arthritis Rheum 2014;66(9):2391–402.
8. Yang X, Harkins LK, Zubanova O, Harrington A, Kovalenko D, Nadeau RJ, *et al.* Overexpression of Spry1 in chondrocytes causes attenuated FGFR ubiquitination and sustained ERK activation resulting in chondrodysplasia. Dev Biol 2008;321(1):64–76.
9. Ornitz DM, Itoh N. The fibroblast growth factor signaling pathway. Wiley Interdiscip Rev Dev Biol 2015;4(3):215–66.
10. Ben-Zvi T, Yayon A, Gertler A, Monsonego-Ornan E. Suppressors of cytokine signaling (SOCS) 1 and SOCS3 interact with and modulate fibroblast growth factor receptor signaling. J Cell Sci 2006;119(Pt 2):380–7.

11. Cho JY, Guo C, Torello M, Lunstrum GP, Iwata T, Deng C, *et al*. Defective lysosomal targeting of activated fibroblast growth factor receptor 3 in achondroplasia. Proc Natl Acad Sci U S A 2004;101(2):609–14.
12. Babon JJ, Nicola NA. The biology and mechanism of action of suppressor of cytokine signaling 3. Growth Factors 2012;30(4):207–19.
13. Greenhalgh CJ, Bertolino P, Asa SL, Metcalf D, Corbin JE, Adams TE, *et al*. Growth enhancement in suppressor of cytokine signaling 2 (SOCS-2)-deficient mice is dependent on signal transducer and activator of transcription 5b (STAT5b). Mol Endocrinol 2002;16(6):1394–406.
14. Cho DC, Brennan HJ, Johnson RW, Poulton IJ, Gooi JH, Tonkin BA, *et al*. Bone corticalization requires local SOCS3 activity and is promoted by androgen action via interleukin-6. Nat Commun 2017;8(1):806.
15. Ono N, Ono W, Nagasawa T, Kronenberg HM. A subset of chondrogenic cells provides early mesenchymal progenitors in growing bones. Nat Cell Biol 2014;16(12):1157–67.